Review Article

Advances in Mechanical Engineering

Advances in Mechanical Engineering
2015, Vol. 7(5) 1–20

DOI: 10.1177/1687814015586120
aime.sagepub.com
SAGE

Recent trends in solar thermal sorption cooling system technology

Khaled M Bataineh and Saja Alrifai

Abstract

Solar thermal cooling is the best alternative solution to overcome the problems associated with using nonrenewable resources. There are several thermal cooling methods developed differing from each other according to the thermodynamic cycle and type of refrigerant used. Recent developments in absorption and adsorption solar cooling systems are presented. Summarized thermodynamic modeling for both absorption and adsorption solar cooling systems is given. Brief thermal analysis among the types of solar collectors is presented. System efficiencies and optimization analysis are presented. The influences of geometrical, system configurations, and physical parameters on the performance of solar thermal sorption cooling system are investigated. The basis for the design of absorption and adsorption solar cooling systems is provided. Several case studies in different climatic conditions are presented. Economic feasibility for both systems is discussed. Comparison between the absorption and adsorption solar cooling system is summarized.

Keywords

Absorption solar cooling systems, adsorption solar cooling systems, air conditioning, solar energy, thermal cooling, economic analysis

Date received: 4 February 2015; accepted: 30 March 2015

Academic Editor: Mohammad Reza Salimpour

Introduction

It is now well known that the nonrenewable sources in the world are finite and they ultimately will be consumed.[1–4] Up to date, 80% of electricity is generated by fossil fuels.[1] Demands on refrigeration and air conditioning have witnessed significant increase recently. Due to environmental awareness and technological advancement, improved standard living, and high oil price, the world is forced to utilize renewable energy sources to meet its growing demand.

Solar cooling can be divided into two main categories: passive and active solar cooling. In passive solar cooling method, the building is protected against heat by blocking sun radiation. The active solar cooling is classified into two categories: using traditional air conditioning system powered by photovoltaic (PV) panels and thermal cooling method. Absorption, adsorption, and desiccant are the main thermal cooling systems. The main advantage of these technologies is the ability to work with environmental-friendly refrigerants and at low temperature.[5–7]

This article aims to provide literature review about recent trends in solar sorption cooling system technology. Detailed description of these technology combined with solar collector will be presented. A number of solar thermal cooling configurations, development, and designs, including the cost and feasibility, are provided and discussed. The results of several case studies located in several locations in the world are presented.

Department of Mechanical Engineering, Jordan University of Science and Technology, Irbid, Jordan

Corresponding author:
Khaled M Bataineh, Department of Mechanical Engineering, Jordan University of Science and Technology, Irbid 22110, Jordan.
Email: k.bataineh@just.edu.jo

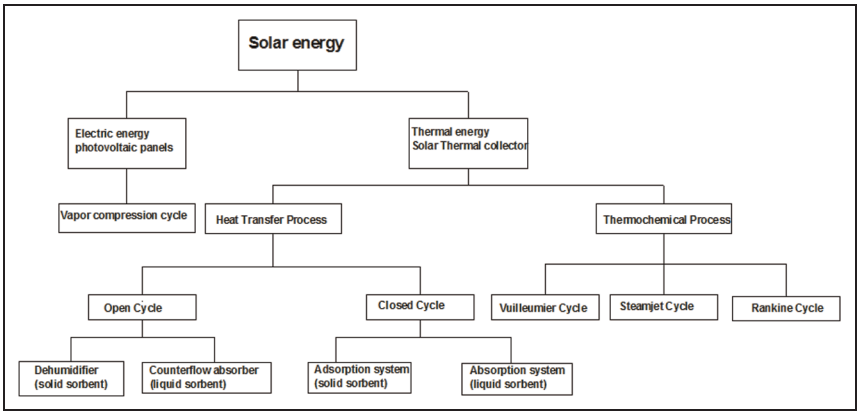

Figure 1. Solar cooling method and the thermodynamic cycle used.

Solar thermal cooling methods

Recently, solar thermal cooling has received significant attention by many researchers. Research has focused on developing methods to meet cooling demand with high efficiency and low cost. There are several types of solar cooling systems found in the literature. Anyanwu[8] and Henning[9] presented classification for solar cooling methodologies summarized in Figure 1. Detailed discussion about absorption and adsorption cooling technologies which used closed cooling cycle will be presented in the next sections. The review will discuss the main cooling mechanism, performance, and economic feasibility. The performance of several prototypes built in several locations in the world is provided.

Solar thermal sorption cooling system technology

Figure 2 shows the basic configuration of solar thermal sorption cooling systems. In the adsorption system, the adsorber is used instead of the absorber. Solar thermal cooling system consists mainly of solar collector, storage tank, condenser, evaporator, heat exchanger, expansion valve, and the refrigeration chamber. The refrigeration chamber in the absorption system is an absorber and in the adsorption system is an adsorber.

Solar thermal technology (solar collector)

Solar cooling utilizes incoming solar radiation to provide a useful cooling effect. Solar cooling is a promising technology because solar radiation is in phase with the demand for cooling. The high solar radiation during summer leads to an increase in the cooling load while cooling system provides greater cooling effect due to high levels of solar radiation.

The solar collector is a special kind of heat exchanger that converts the solar radiation into useful thermal energy. In the solar thermal applications, the solar radiation is absorbed and transferred to the heat transfer fluid. The efficiency of solar thermal cooling system depends on the choice of solar thermal collector. Collector efficiency is defined as the ratio between the absorbed energy and the solar irradiation.[10] Convection and conduction are the two main modes of heat transfer in solar collector.[11] The main three types of solar collectors that are frequently used in thermal cooling technology are given below.

Flat-plate collector. Flat-plate collector (FPC) is a non-concentrating solar collector having simple operation mechanism. The FP solar collector consists of glazing covers, insulation layers, absorber plates, recuperating tubes, and other auxiliaries. Simple operation mechanism is the main characteristics of FPC. Large amount of solar radiation that passes through glass is absorbed by the absorber plate and transferred to the water circulating inside the tubes. The insulation in the solar collector reduces the heat losses.[12] Flat panel collectors typically have low efficiencies due to their limited water temperature outlet.

Evacuated tube collector. Evacuated tube collectors are a non-concentrating solar collector, permanently fixed in position. These types of solar collectors have different mechanisms because it is designed in the form of heat pipe inside a vacuum-sealed tube.[13] Evacuated tube collectors have much higher efficiencies, but relatively low absorber areas. Evacuating the space between the absorber tube and the cover leads to higher efficiency due to reduction in the heat loss through convection and conduction. Hence, evacuated tube collectors can achieve high performance at high temperature due to the combination of a selective surface and preventing convection losses. They collect both direct and diffuse radiation. Their efficiency is higher at low incident

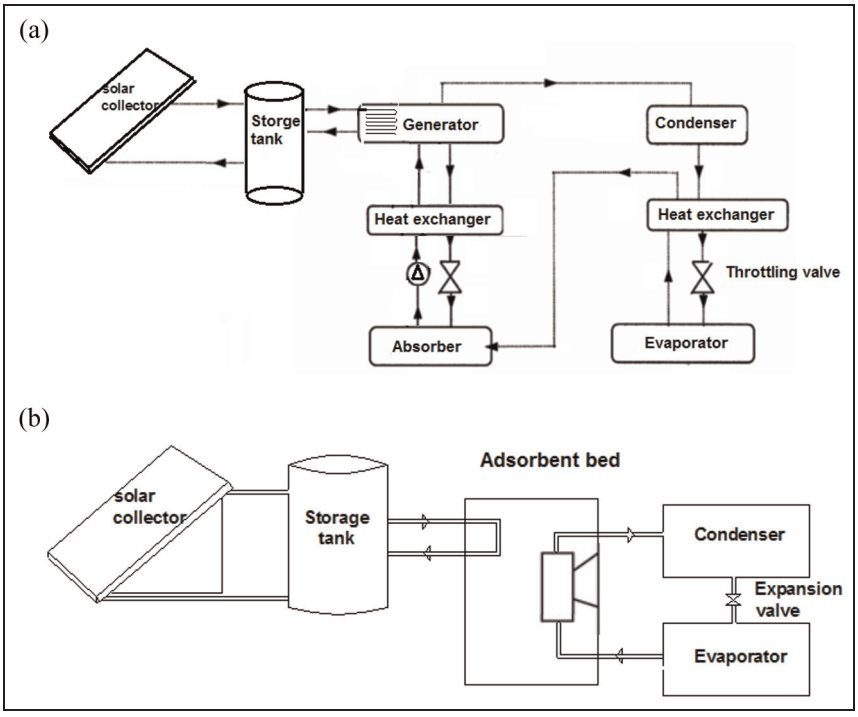

Figure 2. Basic configuration of solar thermal sorption cooling system technology: (a) absorption and (b) adsorption system.

angles. This characteristic gives evacuated tube collector advantages over FPC in terms of day-long performance. The evacuated tube collectors can easily achieve temperature ranges between 70°C and 120°C. A new special class of flat panel collectors is being developed for solar cooling applications. This collector can provide higher temperature than the existing conventional FPC. These collectors have additional insulation and are double glazed, which improves efficiency at the required temperatures. These collectors are expected to be more cost-effective than evacuated tube collectors for solar cooling application.

Concentrating collectors. Concentrating collectors have much higher concentration ratio than the other types. They require sun tracking technology. Different types of concentrating collectors have been developed, that is, Heliostat field collectors, parabolic dish collectors, and parabolic trough collectors (PTCs). Reducing convective and radiative heat losses by using glass and evacuated space between glass and absorber pipe increases the collector efficiency.

Efficient absorption chillers nominally require water of at least 88°C. Flat-plate solar thermal collectors can only produce about 71°C of water temperature. High-temperature flat plate, concentrating, or evacuated tube collectors are needed to produce the required high-temperature water. The performance data presented in Table 1 are indicative and partially based on commercial information. Compared to traditional solar cooling technologies, parabolic trough concentrators can increase the solar cooling efficiency by 40%. As can been seen in Figure 3, using high-temperature solar collectors leads to a significant increase in coefficient of performance (COP) of the absorption chillers cooling system.[14]

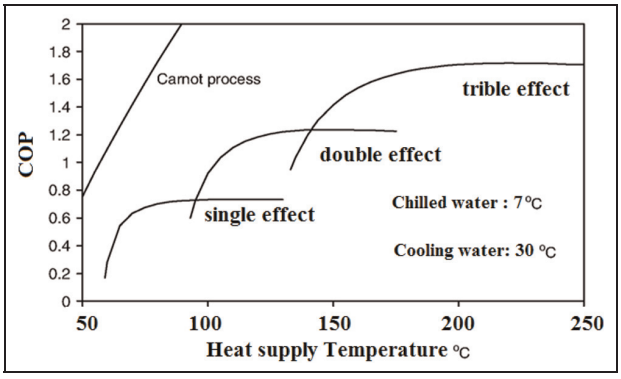

Figure 3. Performance of different types of absorption chillers with solar collector types.[14]

Thermal analysis of solar thermal sorption cooling system

Below are the main equations and steps for designing solar thermal sorption cooling system to meet the cooling demand.

Table 1. Comparison of solar cooling technologies.

	Evacuated tube collectors + single-stage absorption chiller	Parabolic troughs + double-stage absorption chiller collector efficiency	Evacuated tube collectors + triple-effect absorption chiller
Collector efficiency	0.6	0.5	0.6
Chiller efficiency (COP)	0.75	1.34	1.7
Total system performance	0.45	0.67	1.02

COP: coefficient of performance.

Heat transfer in solar collector. The useful collector energy can be calculated from formula suggested by Duffie and Beckman[15]

$$Q_u = A_c \cdot I \cdot \eta_c \tag{1}$$

The performance of a solar collector is described by an energy balance that indicates the conversion of incident solar energy into useful energy gain, thermal losses, and optical losses. Solar collector efficiency is given by[15]

$$\eta_c = F_R \cdot \left[(I_s\alpha) - U_L \cdot \frac{T_{in} - T_{out}}{I}\right] \tag{2}$$

FPC. The useful energy may also be expressed in terms of the energy gained by the absorber and the energy lost from the absorber as[15]

$$Q_u = A_c F_R \left[\alpha\tau I_s(t) - U_L(T_{pm} - T_a)\right] \tag{3}$$

The heat removal factor F_R is defined to relate the actual useful energy gain with fluid inlet temperature T_{fi} given as[15]

$$F_R = \frac{\dot{m}}{A_c}\frac{C_p}{U_L}\left[\frac{T_{fo} - T_{fi}}{\frac{S}{U_L} - (T_{fi} - T_a)}\right] \tag{4}$$

where S is the solar energy absorbed and $\dot{m}$ is the mass flow rate inside the collector (kg/s). The useful energy may also be expressed in terms of the energy gained by the absorber and the energy lost from the absorber as

$$Q_u = A_c F_R[\alpha\tau I - U_L(T_i - T_a)] \tag{5}$$

$$U_L = U_t + U_b + U_s \tag{6}$$

where U_t is the top heat loss coefficient, U_b is the bottom heat loss coefficient, and U_s is the side heat loss coefficient. Their definitions are given in Duffie and Beckman.[15] Detailed presentation about the thermal performance calculations of FPC can be found in Duffie and Beckman.[15]

Evacuated tube collector. The useful energy gained can be evaluated by knowing the inlet and outlet fluid temperatures T_i and T_f and the mass flow rate of water $\dot{m}$ and given as

$$Q_u = \dot{m}C_w(T_f - T_i) \tag{7}$$

The useful energy may also be expressed in terms of the energy gained by the absorber and the energy lost from the absorber as

$$Q_u = A_c F_R[\alpha\tau I - U_L(T_i - T_a)] \tag{8}$$

The heat loss coefficient of the absorber tube is usually calculated based on the following correlation

$$U_L = \frac{\dot{m}C_p(T_i - T_f)_{av}}{A_a(T_m - T_a)_{av}} \tag{9}$$

where $\dot{m}$ is the mass flow rate of water inside the tube (kg/s); C_p is the specific heat of water (J/kg K); T_i and T_f are the inlet and outlet water temperatures, respectively, inside the tube; A_a is the surface area of the absorber; and $(T_m - T_a)_{av}$ is the average difference between the mean water temperature and the ambient temperature over some period of time. Budihardjo et al.[16] showed that heat loss coefficient varies with tube quality. For good quality tubes, the heat loss coefficient varies from 0.5 W/m^2 K (at $T_m - T_a = 25$°C) to 0.65 W/m^2 K (at $T_m - T_a = 65$°C). For lower quality tubes, the coefficient varies from 0.7 to 0.9 W/m^2 K for the same temperature range.[16]

PTC. Typically, the practical concentrating ratio for PTC systems is below 10 defined as[15]

$$CR = \frac{W - d_R}{\pi d_R} \tag{10}$$

where W is the aperture width (m) and d_R is the receiver diameter. The solar radiation absorbed by the receiver S is given as[15]

$$S = I_b \times r_b \times (\tau\alpha)_b\left(\rho \times \gamma + \left(\frac{d_R}{W - d_R}\right)\right) \tag{11}$$

where r_b is the tilt factor; I_b is the beam radiation (W/m^2); ρ is the specular reflectivity of the concentrator surface; γ is the intercept factor, the fraction of the

specularly reflected radiation intercepted by the absorber tube; and $(\tau\alpha)_b$ is the average value of the transmissivity–absorptivity product for beam radiation. The overall heat loss coefficient U_L can be calculated as[15]

$$U_L = \frac{\frac{q_L}{L}}{\pi \times (d_{oa}) \times (T_{pm} - T_a)} \tag{12}$$

where d_{oa} is the outer diameter of absorber tube (m), T_{pm} is the mean temperature of absorber tube (m), T_a (K) is the ambient temperature, and q_L/L is obtained by solving the two equations below

$$\frac{q_L}{L} = h_{p-c}(T_{pm} - T_c)D_o\pi + \frac{\alpha\pi D_o(T_{pm}^4 - T_c^4)}{\left\{\frac{1}{\varepsilon_p} + \frac{D_o}{D_{ci}}\left(\frac{1}{\varepsilon_c} - 1\right)\right\}} \tag{13}$$

$$\frac{q_L}{L} = h_w(T_c - T_a)\pi D_{co} + \alpha\pi D_{co}\varepsilon_c(T_c^4 - T_{sky}^4) \tag{14}$$

where $h_{p\text{-}c}$ is the convective heat transfer coefficient between the absorber tube and the glass cover and h_w is the heat transfer coefficient on the outside surface of the cover. The heat removal factor F', can be calculated as

$$F' = \frac{1}{U_L\left[\frac{1}{U_L} + \frac{D_o}{D_i h_f}\right]} \tag{15}$$

where h_f is the fluid heat transfer coefficient in the absorption tube

$$\frac{(T_{fo} - T_{fi})}{\frac{CS}{U_L} + T_a - T_{fi}} = 1 - \exp\left\{-\frac{F'\pi D_o U_L L}{\dot{m} C_p}\right\} \tag{16}$$

To achieve higher efficiency, PTC requires sun tracking. The most widely used tracking modes for PTC can be summarized as follows:[15]

Mode I: the collector is rotated about a horizontal E–W focal axis and adjusted once every day.
Mode II: the collector is rotated about a horizontal focal E–W axis and adjusted continuously.
Mode III: the collector is rotated about a horizontal focal N–S axis and adjusted continuously.
Mode IV: the focal axis is north–south and inclined at a fixed angle equal to the latitude. The collector is rotated about an axis parallel to the earth's axis with an angular velocity equal and opposite to the earth's rate rotation ($15°h^{-1}$).
Mode V: the collector is rotated continuously about the focal axis which is inclined and oriented to north–south. Also, it rotates about perpendicular axis to this axis.

Storage tank. The temperature for outlet water from the storage tank is given by[17]

$$T_{s,new} = T_{s,old} + \frac{\Delta t}{(m \cdot C_{vw})_s} \cdot [Q_u - Q_L - (U \cdot A)_s \cdot (T_s - T_o)] \tag{17}$$

The thermal capacity of the thermal storage is[17]

$$Q_s = \sum (L_i - Q_o) \cdot \Delta t_i \tag{18}$$

Generator. Generator heat transfer is given by[18]

$$Q_G = m \cdot c_p \cdot (T_{iG} - T_{oG}) \tag{19}$$

Evaporator. The heat transfer through evaporator is[18]

$$Q_e = m_{chill} \cdot c_{pwater} \cdot (T_{ie} - T_{oe}) \tag{20}$$

Chillers. The capacity of the chiller is[19]

$$Capacity_{chiller} = \frac{\sum_{h=1}^{h=24} cooling_{load}}{Hours_{available}} \tag{21}$$

$Hours_{available}$ is the hours where cooling is available.

System COP. The system performance is given as[18]

$$COP = \frac{Q_{ref}}{Q_G} \tag{22}$$

Solar absorption cooling system

Interest in utilizing solar absorption for air cooling increased after the oil crisis in the world after 1971. Research has focused on replacing chlorofluorocarbon (CFC) and hydrochlorofluorocarbon (HCFC) gases due to their harmful environmental effect with NH_3/H_2O pairs.[18,20–22] Absorption system is the dominant solar thermal system due to its high COP which ranges between 0.5 and 0.8 especially with temperature above 80°C.[23,24] However, the COP is still low compared to conventional cooling system which can reach 3.0. The annual performance of absorption system depends on solar collector performance, cooling load scheduling, and absorption chiller dimensions.[25]

The fact that absorption cooling systems can operate at relatively low temperature makes them appropriate for solar energy application. Also, absorption cooling system does not require vibration parts which lead to low noise.[18] The main disadvantage of this system is

that the absorption chiller has narrow operating temperature to function properly.[26]

System mechanism

Absorption chiller mechanism depends on the amount of external heat supply and the internal heat and mass exchange rates between water and LiBr. The operation cycle of the solar absorption system can be summarized as follows:[23]

- Water receives heat by solar collector and is pumped to storage tank and then to the absorption generator to heat the LiBr–H_2O.
- When the LiBr–H_2O is heated, the water (refrigerant) vaporizes and separates from the solution to become superheated.
- The superheated vapor is condensed in the condenser by rejecting heat to the cooling water.
- The resulting liquid from condensation process flows to the evaporator through expansion valve to produce a cooling effect by evaporating the refrigerant. The high concentration solution in the absorber (coming from generator) absorbs the evaporated refrigerant and rejects its heat to cooling water.
- At the end of operation cycle, the low concentration solution is pumped through the heat exchanger to the generator, to preheat this solution.

An external heating unit is sometimes used to power the absorption chiller when solar energy is insufficient (low solar radiation level). Low solar radiation may arise due to the system operational time of day and the meteorological conditions.[26–28] Usually, solar cooling system is designed to provide heating during winter; such systems are called double-effect solar thermal cooling system. Several solar cooling systems have been built in several regions.[20,29–32]

Absorption chiller type for solar-driven air conditioning

The absorption cooling cycle can be modeled in different configurations, that is, the single-effect absorption system, the double-effect absorption system, triple-effect absorption system, and the GAX absorption chiller

The single-effect absorption system consists of a generator, condenser, evaporator, absorber, heat exchanger, pump, and two valves, as can be seen in Figure 2(a). The cycle has two circuits: the refrigerant circuit from generator to absorber and LiBr–water solution circuit from the absorber to generator through the heat exchanger. The single-effect absorption chiller has a simple configuration and requires fewer components in comparison to the other systems. The pressure–temperature diagram of single-effect absorption cycle is shown in Figure 4. This system can be used for air conditioning and freezing at moderate generation temperatures between 80°C and 110°C while obtaining evaporator temperatures between −30°C and −20°C with COPs around 0.60.[32] Llamas-Guillén et al.[33] used evacuated tube solar collector to drive the one-stage ammonia–lithium nitrate air-cooled chiller. The system was successfully operated at ambient temperatures between 25°C and 35°C and produced chilled water at evaporator temperatures below 10°C. Lizarte et al.[34,35] designed single-effect LiBr–water absorption chiller driven by a solar energy using vacuum flat-plate solar collectors. The model is described as a direct air-cooled absorber–condenser. The design aimed to cool air for a 40-m^2 room located in Madrid, Spain. They compared the performance of the indirectly air-cooled single-effect LiBr–water absorption chiller and the directly air-cooled absorption chiller. Both their chiller systems are designed for residential application.

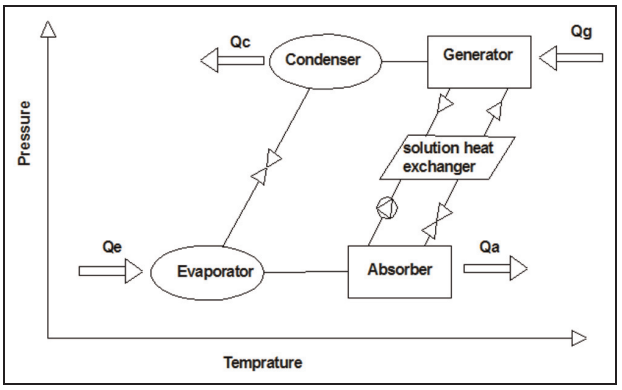

Figure 4. The pressure–temperature diagram of single-effect absorption cycle.

The dynamic analysis of a single-effect LiBr–H_2O absorption chiller was studied by Iranmanesh and Mehrabian.[36] They studied the effect of all thermal masses on various parameters of the absorption chiller. Dynamic model of a small single-effect absorption chiller was developed by Kohlenbach and Ziegler.[37,38] The model is based on the external and internal steady-state enthalpy balances for all system components. They conducted sensitivity analysis based on the variation in model parameters.

Double-effect or double-stage thermo-cycle of LiBr–H_2O system is shown in Figure 5. It consists of high-pressure and the low-pressure stage. Each stage consists of absorber, generator, and heat exchanger. Condensed vapor circulates in high-pressure stage and is transferred to the evaporator in the low-pressure stage. Double-effect cycle is developed to avoid the disadvantages of single-effect chiller and to exploit a low driving

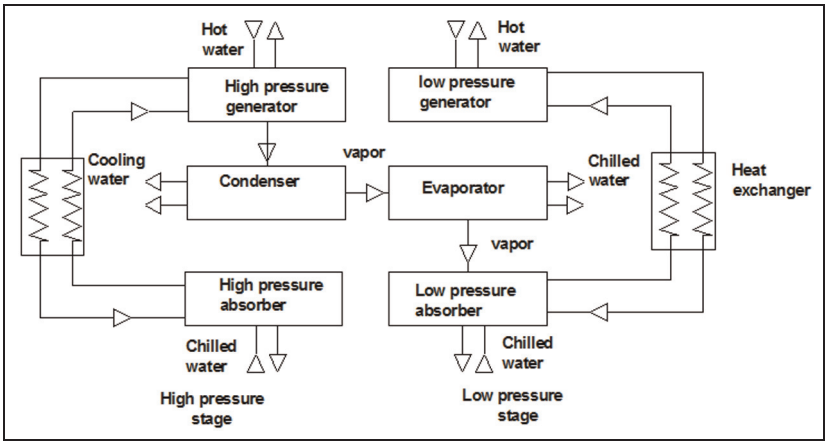

Figure 5. Double-effect absorption cooling system.

temperature in cooling system. This system offers the ability to work under variable solar energy and low levels of solar radiation. Furthermore, reducing the irreversibility of heat transfer can lead to higher COP which could reach twice that of single effect. In general, the double-effect system has a higher performance value and lower cost than the single-effect system.[26,39–41] Double-effect system is able to operate at high condensation temperature T_c which can reach up to 53°C and generation temperature T_g of 80°C to achieve COP of 0.38. On the other hand, single-effect cannot operate at T_c higher than 40°C–45°C.[39]

Du et al.[42] developed air-cooled two-stage NH_3-H_2O system. A 2-kW cooling capacity system was built to investigate the system performance and its feasibility. When the prototype is driven by temperature equal to 85°C of hot water and ambient air temperature of 29°C with evaporating temperature of 8°C, the thermal COP and electric efficacy reach 0.21 and 5.1, respectively. To achieve optimum length of absorption cycle, the low-pressure absorber should be placed a head of double-stage system, while the middle- or high-pressure absorber should be placed at the end. The reason behind this arrangement is that the heat loads of middle-pressure absorber are lower than that of the low-pressure absorber and the efficiency of liquid-interface mass transfer in the middle pressure is higher than that of the low-pressure absorber.[43]

The triple-effect absorption cycle systems are more similar to the single-effect than to that of the double-effect systems. However, the system consists of additional generator, condenser–generator, and heat exchanger. In the triple-effect systems, the refrigerant is produced in three different stages. The triple-effect systems are the most complex compared with the previous systems. Highest COP can be achieved with triple-effect systems with generator temperatures above 150°C.[14,44] Using triple-stage absorption cycle is also investigated by Grossman[41] and found to have higher efficiency

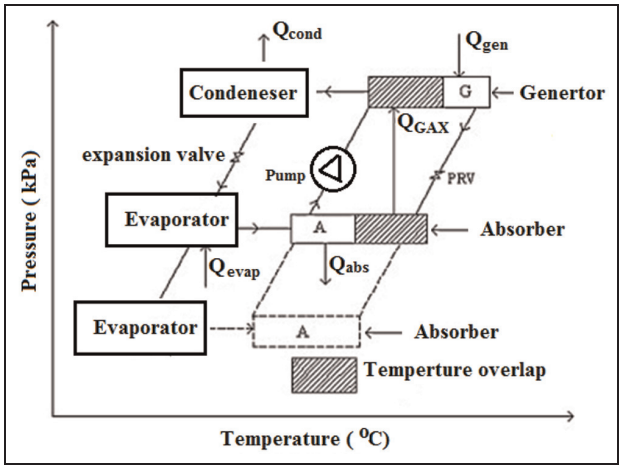

Figure 6. Schematic diagram of GAX absorption cycle.

which is unfortunately accompanied by higher initial cost.

The generator–absorber heat exchange GAX absorption cycle shown in Figure 6 has attracted many researchers recently. The solid line represents the GAX cycle and the dotted line represents the single-effect cycle. Higher COP of the GAX cycle can be achieved due to the existence of temperature overlap. This overlap occurs between the absorber and the generator as a result of maintaining the pressure and concentration in the absorber and generator. The GAX cycle can be used with ammonia–water and cannot be used with lithium bromide–water absorption cooling system. Jawahar and Saravanan[45] presented a comprehensive review of several different GAX cycle configurations and their performance. Their study showed that an improvement in the COP of about 10%–20%, 20%–30%, and 30%–40% in absorber heat recovery cycle, simple GAX, and branched GAX cycle, respectively, than that of a conventional single-effect system for the same set of operating conditions. Yari et al.[46] performed energy and

exergy analyses of ammonia–water GAX absorption cycles. They conducted parametric analysis using EES software to investigate the effect of design parameters in the system components. Velázquez and Best[47] performed thermodynamic analysis for air-cooled GAX system. The system was driven by solar energy and hybrid natural gas. For ambient air up to 40°C with a relative humidity (RH) of 24% as cooling source, the COP of cooling and COP of heating and the heat recovery were found to be 0.86, 1.86, and 16.9 kW, respectively. Zheng et al.[48] simulated GAX cycle and single-stage ammonia absorption system. They used the concept of exergy coupling to study the cycles. The absorption cycle was divided into the heat engine and heat pump subcycles for thermodynamic analysis. The results of the study showed that the exergy demand of the heat pump subcycle in the GAX cycle and the exergy demand of the single-stage cycle was the same.

The ranges of generator temperature requirements using single effect or double effect are different. The generation temperatures from 110°C to 140°C are too high for a single-effect chiller and not enough to drive a double-effect LiBr–water absorption chiller. For this reason, the absorber generator heat exchanger AGX was added to the LiBr–water absorption chiller in the study conducted by Xu et al.[49] The new cycle containing AGX is able to work under generation temperatures between 85°C and 150°C with 40°C condensation temperature, 5°C of evaporation temperature, and 35°C of absorption temperature. The COP for the AGX cycle with generation temperatures of 93°C–140°C ranges between 0.75 and 1.08. Xu and Wang[50] studied experimentally the AGX cycle using LiBr–water. Their experimental results show that the COP of the AGX absorption chiller ranges between 0.69 and 1.08 under generation temperature between 95°C and 120°C.

Thermodynamic modeling

Figure 4 shows the absorption cycle pressure–temperature. Thermodynamic model of the cycle is developed under the assumptions of steady-state conditions, heat losses and pressure drops in the tubes components are negligible, adiabatic expansion valves, isentropic pump, solution leaves the absorber and generator are saturated, refrigerant at the evaporator and condenser outlets are saturated.[23]

The thermodynamic modeling of the thermophysical processes occurring in various parts in the refrigeration unit can be summarized as follows:

- *Evaporator and condenser*
  The temperature variations in both heating and cooling fluids on the evaporator and condenser are determined by multi-variable polynomials obtained by the differential equations of heat transfer.[51]
  The total heat transfer rate through the condenser surface area is given by[51]

$$\int_{Acon} dQ = Q_{con}(m_{abs}, P_{abs}, T_{des,o,o}, T_{abs,o}) = m_{abs}\left(h_{con,o}(P_{con,o}, T_{con,o}) - h_{abs,o}(P_{abs,o}, T_{abs,o})\right) \tag{23}$$

  The total heat transfer rate through the evaporator surface area is given as

$$\int_{Aevap} dQ = Q_{evp}(m_{con,o}, P_{abs}, T_{con,o}) = m_{evap,i}\left(h_{evap,i}(P_{evap,i}, T_{evap,i}) - h_{evap,o}(P_{evap,o}, T_{evap,o})\right) \tag{24}$$

- *Absorption chillers*
  The absorption chiller consists of desorber and absorber; the heat and mass transfer through the absorption chillers is governed by[51]

$$\int_{Aabs} dQ = Q_{abs}(m_{des,o}, m_{abs,o}, m_{abs,i}, \chi_{des,i}, P_{abs,subcooled,o}, T_{abs,i}) = m_{abs,i}\left(h_{abs,o}(P_{abs,o}, T_{abs,o}) - h_{abs,i}(P_{abs,i}, T_{abs,i})\right) \tag{25}$$

$$\int_{Aabs} d_{mvap} = m_{vap,abs}(m_{des,o}, m_{abs,o}, m_{abs,i}, \chi_{des,i}, P_{abs,subcooled,o}, T_{abs,i}) = m_{evap,vap,o} \tag{26}$$

- *Generator*
  Energy balance of the generator is developed under the assumption of isobaric conditions with respect to the condenser and refrigerant heat exchanger. The equations of energy balance of the generator are derived under local thermodynamic equilibrium condition within the various phases[52]

$$\frac{dQ_{gen}}{dT_{gen}} = m_{vapCp}\left(P_{gen}, T_{vap}, y_{vap}(P_{gen}, T_{vap})\right)\frac{dT_{vap}}{dT_{gen}} - m_{solCp}\left(P_{gen}, T_{gen}, x_{sol}, (P_{gen}, T_{gen})\right) + \sum_{i=1}^{2}\frac{\partial H}{\partial m_i}\left(P_{gen}, T_{gen}, y_{vap}(P_{gen}, T_{vap})\right)\frac{dm_{i,vap}}{dT_{gen}} - \sum\frac{\partial H}{\partial m_i}\left(P_{gen}, T_{gen}, x_{sol}(P_{gen}, T_{gen})\right)\frac{dm_{i,sol}}{dT_{gen}} \tag{27}$$

The energy balance for the falling-film absorber is modeled under the assumptions of isobaric condition in the evaporator, refrigerant heat exchanger, air-cooled absorber, and solution-cooled absorber. The evaporator pressure drop resulted in lowering absorber pressure which results in reduced absorption process efficiency; GAX absorber type was adopted in modeling by[52]

$$\begin{aligned}\frac{dQ_{abs}}{dT_{abs}} = & -m_{vapCp}(P_{abs}, T_{vap}, y_{vap})\frac{dTvap}{dT_{abs}} \\ & -m_{solCp}(p_{abs}, T_{abs}, x_{sol}) \\ & -\sum_{i=1}^{2}\frac{\partial H}{\partial m_i}(P_{abs}, T_{vap}, y_{vap})\frac{dm_{i,vap}}{dT_{abs}} \\ & -\sum_{i=1}^{2}\frac{\partial H}{\partial m_i}(P_{abs}, T_{abs}, x_{sol})\frac{dm_{i,sol}}{dT_{abs}}\end{aligned} \quad (28)$$

An external heating unit sometimes is used to power the absorption chiller when solar energy is insufficient (low solar radiation level). Low solar radiation may arise due to the system operational time of day and the meteorological conditions.[53–56] Usually, solar cooling system is designed to provide heating during winter; such systems are called double-effect solar thermal cooling system. Several solar cooling systems have been built in different regions.[20,29–32]

System efficiency

Solar absorption systems are considered more reliable, quiet, and feasible than the adsorption system. The high initial cost and low efficiency prohibit their commercial spread. These facts motivate large number of studies aimed to overcome these drawbacks. The system efficiency has improved by using high-temperature solar receiver, double-effect chiller, advanced control, and improved chiller efficiency.[53] Hang et al.[30,54] investigated the system performance by using linear regression model and central composite design. Their analyses showed that the economic performance is inversely proportional to the thermal system performance.[54] Atmaca and Yigit[17] investigated the effect of several parameters (inlet generator temperature, surface area of absorber and heat exchanger, volume of storage tank) on system performance. They found that COP increases with increasing generator inlet temperature and increasing surface area of both absorber and heat exchanger. The optimal temperature for highest COP corresponds to 80°C. Also, increasing thermal storage tank volume leads to higher daily cooling production.[22]

System performance increases with increasing water storage tank temperature. Utilizing water storage tank allows continuous operation and increased system reliability.[55] Storage tank usually requires flow control.[56] Design of storage tank and thermal stratification plays an important role in the system efficiency. Stratified storage tank achieves higher heat output and higher COP than the conventional fully mixed storage tank that can be obtained by using multi-node inside the tank with variable inlet temperature.[57,58] Because LiBr–H_2O absorption chiller can operate at high temperature reaching boiling temperature, the volume of the storage tank must be designed properly to prevent energy loses by maintaining the temperature close to the chiller operating temperature.

Outdoor temperature has significant effect on the COP of the chiller, especially when the dry cooling tower is used to evacuate the absorption heat. To remove this negative effect on chiller COP, Palacin et al. used open geothermal cycle as a heat rejection tank.[59] Eicker et al.[60] made comparison study between geothermal, wet, and dry geothermal heat rejection tank and found that the electrical COP is between 4 and 8 when using dry heat rejection.

Due to the several external irreversibities such as heat conduction, mass transfer, friction, eddy, and others, the performance cannot reach high values. Also, internal irreversibility such as heat engine cycle/generator–absorber and refrigeration cycle/evaporator–condenser has higher impact on reducing the performance.[61] Fathi et al.[62] studied the impact of irreversibility on solar absorption refrigerator by using four reservoir models; each of them has internal and external irreversibilities operated at the maximum cooling load. They compared their modeling results with single-stage system using semi-empirical model. Their results show that both models predict similar values of COP.

Table 2 summarizes the performance of the solar cooling system using LiBr–H_2O as an absorption chiller under different climate and operation conditions and different parameters.

Several studies have investigated the thermal and the economical assessment of solar cooling absorption system in several regions. Marc et al.[68] presented an experimental study of a solar cooling absorption system implemented in Reunion Island, located in the southern hemisphere near the Capricorn Tropic. Indoor thermal comfort is achieved by a self-stabilizing operating system that maintains the indoor temperature 6°C below the outdoor temperature. Assilzadeh et al.[55] designed solar cooling system suitable for Malaysia and similar tropical regions using evacuated tube solar collectors and LiBr absorption unit. TRNSYS is used to simulate the absorption solar cooling system for weather data for Malaysia. A continuous operation is achieved by utilizing a 0.8-m^3 hot water storage tank. They found that the optimum system for Malaysia's climate for a 3.5-kW (1 refrigeration ton) system consists of 35-m^2 evacuated tubes solar collector sloped at 20°. Eicker

Table 2. Solar absorption summarized results.

Ref. No.	Solar collector		Absorption chiller (kW)	Storage capacity (m^3)	Solar fraction (%)	Collectors efficiency (%)	COP	Prototype location
	Type	Area m^2						
26	VT	96	8	3	43.5	–	0.31	Shanghai
27	VT	72	35	–	81	–	–	Thailand
28	FP	50	6–10	0.040/m^2 of FP	56	–	–	Spain
41	FP	500	100 (2 stages)	–	–	55	0.38–0.43	South china
55	VT	35	3.5	–	0.8	–	–	Malaysia's climate
63	VT	108	35.17	1.5	31.1–100	35.2–49.2	0.37–0.81	Oberhausen, Germany
64	FP	30	11	0.8	–	–	0.61–0.725	Tunisia
65	Fresnel collector	352	134	75%	75	35–40	1.1–1.25	Seville
66	FP	49.9	35	2	–	50%	0.42	Madrid, Spain
67	FP	37.5	4.5	0.700	–	–	0.46–0.6	Zaragoza (Spain)

COP: coefficient of performance; FP: flat plate; VT: evacuated tube.

and Pietruschka[25] presented a full simulation model for absorption cooling systems, combined with a stratified storage tank, steady-state or dynamic collector model, and hourly resolved building loads for several locations in Europe. They found that the control strategy, recooling temperature levels, location, and cooling load time series have a strong influence on the solar thermal system design and performance. Their results showed that between 1.7 and 3.6 m^2 of vacuum tube collectors per kilowatts cooling load are required to cover 80% of the cooling load. Their cost analysis showed that Southern European has significantly lower costs. For long operation hours, cooling costs are estimated to be around 200 and about 280 € MW/h for buildings with lower internal gains and shorter cooling periods, respectively. For a Southern German climate, the costs are more than double. Ghaddar et al.[69] developed a simulation program for modeling and performance evaluation of the solar-operated lithium bromide absorption system for all possible climatic conditions of Beirut, Lebanon. The results indicated that a collector area of 23.3 m^2 with water storage tank capacity ranging from 1000 to 1500 L is required for each ton of refrigeration. Their economic assessment revealed that the solar cooling system is marginally competitive only when combined with domestic water heating. Tiago and Oliveira[31] evaluated the potential of integrated solar absorption cooling and heating systems for building applications for three different locations and climates: Berlin (Germany), Lisbon (Portugal), and Rome (Italy). Their results revealed that integrated solar absorption cooling and heating systems have potential to save total cost and CO_2 emission, and it is more attractive when natural gas is used as system backup energy. The energy performance depends on the building type and location. Jaruwongwittaya and Chen[70] found that solar-powered absorption chiller in Thailand can save electricity up to 7882 kW h/year/ton of refrigerant (TR), and this accounted for 98.56% of total electricity consumption of vapor compression system. Shekarchian et al.[71] investigated the annual energy required for cooling per unit area and the total energy cost per unit area for both vapor compression and absorption systems in different climates in Iran. Their results showed that using absorption chiller increases the energy consumption per unit area, but it decreases the energy cost per unit area of cooling. Furthermore, they showed that increasing the COP of absorption chiller by 0.1, at least \$50 m^{-2} of energy cost saving can be achieved. Trygg and Amiri[72] revealed that by switching from conventional vapor compression chiller to heat-driven absorption chiller in a combined heat and power (CHP) system in Swedish municipality, the production cost of cooling can be reduced by 170%.

Economic feasibility

Economic viability and technological maturity are the main factors affecting the commercializing of cooling system. Economic viability depends on many factors such as the energy policy and guidelines, price of oil, and price of solar collector. High system cost is mainly due to high initial cost of solar collector and absorption chiller, and chiller technical problems.[21,73]

There are several measures to determine the economic feasibility of the solar cooling system. Payback period (Pb), net present value (NPV), present worth value, cost of unit energy, and cost of primary energy (PE) saved ($C_{p,saved}$) are the most economic indicators used. The Pb is given by[74]

$$Pb = \frac{\log\left[\frac{C}{E} \cdot \frac{i}{100} + 1\right]}{\log\left(1 + \frac{i}{100}\right)} \tag{29}$$

The NPV is given by[74]

$$NPV = Y \cdot \frac{1}{r-i}\left[1-\frac{1+i}{1+r}\right]^{L} - C_c \quad (30)$$

The cost of PE saved ($C_{p,saved}$) is given by[74]

$$C_{p,saved} = \frac{\Delta C_{annual,sol}}{PE_{saved}} \quad (31)$$

The present worth value, which is the indicator to the value of system today including the solar collector cost, heat rejection cost, operating cost, and machine cost, is given by[74]

$$pw = A_o\left[\frac{1-\frac{1}{(1+i)^n}}{i}\right] \quad (32)$$

The annual cost comparison method is another economic indicator that includes the solar collector cost, heat rejection cost, operating cost, and machine cost and is given by[74]

$$EA_c = P_c\left[\frac{i(1+i)^n}{(1+i)^n-1}\right] \quad (33)$$

A study conducted in 2003 for cooling system according to Greece price and climate condition found that the Pb of absorption system exceeds the lifetime of system, but NPV is positive.[73] Boopathi Raja and Shanmugam[18] studied the cost of solar absorption cooling system. They found that the absorption system with LiBr–H_2O as a working fluid is more reliable and economical under specific configurations and operational conditions; that is, flat plate with evacuated tube solar collectors, using only three electrical equipments (condenser fan, cooling coil fan, and a pump), minimal heat losses, and increasing vacuum pressure.

Up to now, solar cooling systems are more expensive than conventional cooling systems. To overcome this problem, researchers aim to improve system performance. Regression analysis method is used to increase the cooling system performance when constrained with limited budget.[30,54] Regression analysis method considers relations between several important factors such as solar fraction, area and slope of solar collector, and volume of cold and hot storage tank. Gebreslassie et al.[75] used seven different types of solar collectors for ammonia absorption system using NH_3/H_2O under Barcelona, Spain, climatic conditions. Their work aimed to minimize the environmental impact and the total cost by using a bi-criteria mixed-integer nonlinear programming (MINLP). Tiago and Oliveira[31] designed a combined cooling and heating solar system with gas boiler backup or electrical compression backup. They conducted cost comparison study between conventional solution (gas boiler and electrical compression) and solar system for three different locations. The results vary from one location to another with varying backup and solar collector used. The results showed that the system in single-family house and hotel have a higher economic feasibility. Using vacuum tube collector outperforms the FPC in terms of space and cost.

Tsoutsos et al.[73] used a TRNSYS program to design the LiBr–H_2O absorption cooling system in a Greek hospital. The aim of their study is to provide optimum sizing of system component to provide the heating and cooling demand. The main advantage of their system is high environmental benefit, but the investment has long Pb of 11.5 years. Mehr et al.[76] carried out thermoeconomic performance comparison between GAX absorption cycle and a hybrid GAX absorption cycle (HGAX). The HGAX differs from the GAX that it uses a compressor to raise the absorber pressure. The cycle's performance was optimized based on the exergy efficiency, COP, and the cost of unit product. Better performance and higher unit product cost for HGAX cycle were achieved compared to GAX. At the same operating conditions, the cost of the HGAX cycle was \$180.5 GJ^{-1}, while the cost of standard GAX cycle was \$159.1 GJ^{-1}.

Adsorption solar cooling system

Adsorption solar cooling system is considered the second major system of thermal solar cooling. The work on adsorption solar cooling system started in 1980s where it began with ice making, then making chilled water, and ended up in air conditioning. The adsorption solar cooling is found very suitable for grain storage applications.[71,72,77]

System efficiency depends on the range of temperature source 55°C–300°C and different adsorption working pairs. The cooling method, adsorption properties, and theories on adsorption cycle have been investigated to achieve high performance and low cost.[8,78,79] Similar to absorption system, adsorption system offers several advantages such as ability to work with wide range of driving temperature levels, noiseless operations, simple control, and absence of corrosion problem.[79–81] The long adsorption/desorption time, the size of the system, high cost of adsorption chillers, and low performance of the adsorption chiller prohibit significant commercial growth. This system differs from the absorption system in that they need two or more absorbers to provide continuous operation.[73] Furthermore, they need a well-designed solar collector and desorber with good heat release characteristics to achieve good efficiency.[82]

Many adsorbent–refrigerant pairs have been used in cooling system such as activated carbon–ammonia, activated carbon fiber–methanol, activated carbon–ethanol, zeolite–water, silica gel–water, and calcium chloride–ammonia.[82,83] Choosing the adsorbent–refrigerant pair is a crucial step in system design.

Several criteria have been considered when choosing the best refrigerant, such as low cost, low toxicity, large vaporization enthalpy, working pressure, low freezing temperature, chemical stability, and small molecular dimensions. Heat losses can be avoided by using refrigerants having large vaporization enthalpy.[84,85] Activated carbon pairs are widely used because of their properties such as micro pure volume and high surface area.

Anyanwu and Ogueke[86] carried out a comparison study between three adsorption pairs and found that the adsorption system is considered poor thermal system. Using zeolite–water, COP is about 0.3 which is higher than COP of using activated carbon–methanol and activated carbon–ammonia. The silica gel–water is able to work at a temperature below 100°C, that is, 55°C–95°C with COP equal to 0.403. This refrigerant has no crystallization problem and no corrosion problem. The systems using silica gel–water do not require solution pump.[87,88]

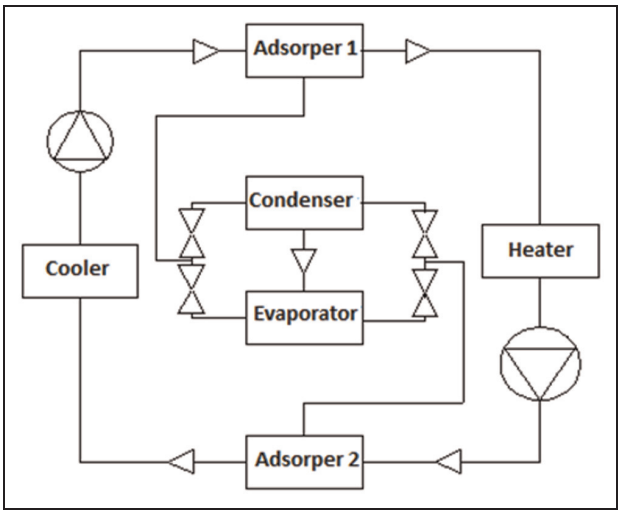

Figure 7. Schematic diagram of heat recovery silica gel–water two-bed adsorption chiller.

System mechanism

Solar adsorption systems are classified according to the cycle used: the intermittent cycle and continuous cycle. Despite their technically success of intermittent cycle, but its high cost limits their spread and will not be further discussed. On the other hand, continuous cycle system is widely used because of its ability to produce refrigeration and cooling. There are several technologies implementing adsorption continuous cycles, thermal wave adsorption technology,[89] convective thermal wave adsorption technology,[90] and multi-stage and cascading technology.[91,92]

The solar adsorption cooling consists mainly of solar collector array, heat storage tank, chillers, pumps, fan coil unit, cooling tower, and several valves as shown in Figure 2(b). The chiller mechanism is explained in Alghoul et al.,[84] Ge et al.[92] and Wang and Oliveira.[93] The adsorption chiller has been designed using one bed, two beds, or multi-beds. However, the adsorption chiller using two-bed configuration is the most widely used. In the two-bed chiller system, evaporation and condensation of water in the hot and cold champers cause heat and pressure changes between two beds. This process has three phases consequently: (1) the adsorption/desorption phase, (2) the mass recovery phase, and (3) the heat recovery phase. Detailed descriptions of these phases are presented in Ge et al.[92] Figure 7 shows the schematic diagram of the two-bed adsorption chiller consisting of evaporator, condenser, valves, and two adsorption beds. The cycle of the system begins with refrigerant at adsorber 2 which is heated by solar energy and transferred to the condenser in order to reach the heating–desorption condensation state. Then, adsorber 1 which is connected to the evaporator is cooled to gather the adsorption refrigeration in it. The condensed liquid flows through the valve toward the evaporator to release adsorption refrigeration in it. The heater and cooler are used in this model as a pump in the circuit to drive thermal fluid.

Thermodynamics modeling of system component

Heat and mass transfer plays a crucial role in determining the performance of the adsorption cooling system. The increase in the performance of the adsorber heat will increase the total adsorber heat transfer coefficient and enhance the heat transfer rate between the heat media and the adsorbent. Increasing the performance of mass transfer will reduce the refrigerant diffusion time in adsorbent and shorten the adsorption–desorption time. This leads to an improvement in the system solar cooling power (SCP).[85]

- *Adsorbent bed*
  The combination of the heat equation with the mass transfer balance in the adsorbent bed is given as[94]

$$\left[(1-\varepsilon)\cdot\rho_s\cdot C_s+\theta\cdot\rho_a\cdot C_a\cdot(\varepsilon-\theta)\cdot\left(\rho_g\cdot C_{vg}+\frac{P}{T}\right)\right]\frac{\partial T}{\partial t}=K_{ef}\cdot f\left[\frac{\partial 2T}{\partial r2}+\frac{1}{r}\frac{\partial T}{\partial r}\right]+(\varepsilon-\theta)\frac{\partial p}{\partial T}+\theta\cdot\left(\frac{P}{\rho_a}+\Delta H\right)\frac{\partial \rho_a}{\partial t}+\rho_a\cdot\Delta H\frac{\partial\theta}{\partial t} \quad (34)$$

- *Evaporator and condenser*
  Energy conservation equation of the condenser

is given by[95]

$$\begin{aligned}&[m_{cond}\cdot c_{cond}+M_d(t)c_d]\frac{\partial T_{cond}}{\partial t}\\&=m_d(t)\left[L_v(P_{cond})+C_{p.gc}(T_{gc}-T_{con})\right]\\&-A_{cond}\cdot h_{cond-amb}(T_{cond}-T_{amb})\\&-\frac{\sigma\left(T_{cond}^4-T_{amb}^4\right)}{\left(\frac{1}{\varepsilon_c}+\frac{1}{\varepsilon_{amb}}-1\right)A_{gc}}\end{aligned}\tag{35}$$

The mathematical model of energy balance inside the condenser is given under the thermodynamic condition of desorption beds and the difference between the evaporator and the condenser. The condenser energy balance is expressed as[95]

$$\begin{aligned}&(M\cdot C_p)_{cond}\frac{dT_{cond}}{dt}\\&=\phi\left(h_{fg}\cdot M_{ref}\frac{dw_{des}}{dt}\right)\\&-(m\cdot C_p)_w\cdot(T_{w,o}-T_{w,i})\end{aligned}\tag{36}$$

The mass and heat transfer occurring between the adsorption bed and evaporator governed the evaporator energy balance. The evaporator energy balance is expressed as[95]

$$\begin{aligned}&(M\cdot C_p)_{evap}\frac{dT_{evap}}{dt}=\phi\left(h_{fg}\cdot M_{ref}\frac{dw_{ads}}{dt}\right)\\&-(m\cdot C_p)_{chill}\cdot(T_{chill,o}-T_{chill,i})\end{aligned}\tag{37}$$

Solar adsorption system application

Adsorption cooling system is used for many purposes, that is, ice making and refrigeration and air conditioning.

Ice making. Maggio et al.[96] used solar adsorption system for application of ice making. They used the composite sorbent "lithium chloride in silica gel pores." The theoretical COP was 0.33 and the maximum daily ice production was 20 kg/m^2. These results obtained for ice maker used 36 kg of adsorbent material and equipped with a solar collector area of 1.5 m^2. Li et al.[97] used two different working pairs: the activated carbon–ethanol and the activated carbon–methanol in solar ice maker. Their experimental results showed that the activated carbon–ethanol cannot be used in ice making, while the activated carbon–methanol was appropriate for ice making. Hildbrand et al.[98] used silica gel–water in their experimental setup. The system consists of cylindrical tubes used as a solar collector (flat-plate, 2-m^2 double glazed), an adsorber system, a condenser utilizing natural convection air-cooled, and 40 L of evaporator container. The COP values range between 0.10 and 0.25 with a mean value of 0.16. Vasta et al.[99] simulated an adsorptive ice maker that used active carbon–methanol as the working pair. The thermodynamics cycle was developed for all system components: adsorbent bed, solar collector, evaporator, and condenser. The simulation results showed that during all days of June, the ice maker is able to freeze 5 kg. During the months of February and March, the average monthly daily ice production is about 4 kg, while for January, November, and December the daily ice production was 2.0–3.5 kg. The average monthly solar COP varies from 0.045 in July to a maximum of 0.11 in January, with the annual mean COP of 0.07.

Refrigeration and air conditioning. Solar adsorption refrigeration systems are used to meet the needs for refrigeration requirements. Al Mers et al.[100] modeled a solar adsorption refrigerator. The model describes the mass and heat transfer in the cylindrical finned reactor. Giving the meteorological data as boundary conditions on the reactor, the model predicted COP of about 0.105. The model was validated with the experimental results. Louajari et al.[101] studied the effect of a cylindrical adsorber on the solar adsorption refrigerating system performance. The solar energy was used to heat the adsorber that contains an activated carbon–ammonia pair. The adsorber was composed of many cylindrical tubes with external fins. It was found that the mass cycled in the adsorber equipped with external fins is more significant than the adsorber without fins. The optimal diameter of the adsorber with fins is greater than the adsorber without fins. The maximal temperature reached in the adsorber with fins is around 97°C while in the adsorber without fins reached 77°C. Abu-Hamdeh et al.[102] developed adsorption refrigeration model driven by PTC and uses olive waste as adsorbent with methanol as adsorbate. The system was designed and employed as a cooler unit and refrigerator that is suitable for remote areas. This was used to power the system. System performance was calculated in the form of COP, cooling production, COP. They used statistical and experimental methods to achieve the optimum parameters. It was found that the lowest temperature in the refrigerated space was 4°C and the equivalent ambient temperature was 27°C, and COP equals 0.75.

System efficiency

High COP and SCP can be achieved by increasing heat and mass recovery and by developing multi-stage and multi-bed technologies. Yong and Sumathy[95] classified the mathematical models used in the heat and mass transfer analysis process in the adsorption bed into three models: the lumped parameter model, heat and

mass transfer model, and thermodynamic model. The lumped model focuses on the adsorbent bed without considering the bed geometry and expressed mathematically by ordinary differential equations. The heat and mass transfer model focuses on the energy analysis, expressed by partial differential equation. This model allows investigating the effect of different operating and geometric parameters on the COP. The thermodynamic model is used to study the impact of heat transfer and temperature on the COP of the system and is given by algebraic equation.

The general equation used to calculate the COP of adsorption cooling system is[8]

$$COP = \frac{T_e(T_g - T_a)}{T_g(T_a - T_c)} \tag{38}$$

Equation (25) shows that the COP depends on three parameters: evaporating temperature T_e, generating temperature T_g, and ambient temperature T_a. Liu and Leong[103,104] studied the effect of operating condition such as heat exchanger fluid velocity; adsorption temperature T_{ad}, T_g, T_c, and T_e; and heat exchanger fluid temperature $T_{h,in}$ on the performance of adsorption cooling system using zeolite 13X/water. They considered the limitation of mass and heat transfer. They found that the T_{ad}, T_g, T_c, and T_e have a significant effect on system performance, T_{ad} and T_g have an optimal value, the fluid velocity has positive effect on optimal cooling power, and $T_{h,in}$ has no effect on system performance. No large changes in pressure during the heat and mass recovery in absorber were found.[92] The COP can be increased by decreasing the cold water inlet temperature to bed and increasing flow velocity. The inlet hot water temperature has an optimal value to achieve the highest COP. Furthermore, it was found that heat recovery can improve the COP of the system, while mass recovery can improve both the COP and cooling capacity.[104–106] It was found that the system performance increases with increasing adsorbent mass.[107]

The main reasons behind lower values of COP and SCP are heat losses from adsorber during cooling cycle and non-adsorbing mass. To minimize these problems, Lambert[108] modified the absorption cooling system by (a) magnifying the contact area between adsorbent material and heat exchanger and (b) reducing the thickness of effective adsorption to parts of millimeter to overcome the low conductivity. Improved thermal conductivity of the adsorption bed reduced the time required to conduct heat from the outside to the inside bed which leads to higher heat transfer rate. Using ripped plate has a higher heat transfer performance compared to the plate adsorption bed. This is due to the ability of ripped bed to reduce heat losses and distribute heat inside bed. It was found that using thin tube has a higher performance than the performance tubular adsorption bed.[109] The design of adsorption bed usually utilizes fins to reduce the heat resistance between the metal and adsorbent materials and enhance the heat transfer.[94]

In order to optimize the performance of system, Khattab[105,110] added a small piece of blackened steel to the charcoal–methanol solid adsorption pair and covered the bed of glass shell. These additives enhanced the heat transfer inside the sorption bed and increased the COP from 0.146 to 0.1558 and bed efficiency from 55.2% to 58.5%.

Louajari et al.[101] studied the effect of the cylindrical absorber geometric shape (tube diameter and external fins length) on the performance of the cooling system using activated carbon–ammonia pairs.

Mass recovery phase plays an important role in system performance; an investigation of this phase is conducted by Khattab[110] using three-bed silica gel adsorption chiller. They found that the cooling production of the system with mass recovery chiller is higher than that without mass recovery when the temperature of heat source ranges between 60°C and 90°C. Luo et al.[111] used heat and mass recovery phase in silica gel adsorption chiller operating out-of-phase to improve efficiency and allow continuous cooling production. They incorporated methanol evaporator into two water evaporators by using the gravity heat pipe concept. Increasing the mass flow rate of cooling water through condenser increases the COP and specific cooling power SCP[110,111] (Table 3).

Economic feasibility

Solar systems have a high initial cost and low operational cost. The economic feasibility was investigated by considering the Pb, the NPV, energy saving, and operation and maintenance cost. Tsoutsos et al.[73] found that the NPV of cooling system is negative and the Pb of the system exceeds the lifetime according to Greece prices in 2003. The initial cost of the adsorption system is high compared to the conventional system. However, adsorption system is still attractive due to the fact that conventional system has running cost of fossil fuel, electricity transmission cost, energy conversion cost, and system maintenance cost. The adsorption pairs such as zeolite–water and activated carbon–methanol are very expensive and prevent market growth despite their technical success. An increase in the geometrical construction such as width pipe increases the cost; on the other hand, simplified or reduced construction will reduce the cost.[77,112] Chang et al.[83] used a vacuum tank containing evaporator condenser and adsorption bed to reduce the manufacturing cost and achieve high efficiency.

Table 3. Solar adsorption system results.

Ref. No.	Solar collector		Adsorption chiller output	Adsorption pairs (kg)	No. of beds	Storage chilled capacity (m^3)	Solar radiation (locations)	Collector efficiency (%)	Solar cooling COP
	Type	Area (m^2)							
24	FT	10.5	500 W	Theoretical study	1 bed	–	900-1200 W/m^2	–	0.23
91	VT	150	8.5 kW	Silica gel	2 chillers	2.3	18.5 MJ/day m^2 (Shanghai)	–	0.35
84	VT	–	12 kg/day	12 kg activated carbon–methanol	2 beds, dual purpose	–	61.2 MJ/day m^2	–	0.44
111	VT	49.4	3.2–4.4 kW	Silica gel 50 kg	1 bed	0.03	16–21 MJ/day m^2	–	0.1–0.13
106	FT	3.5–4.5	10 kg/day	50–60 kg activated carbon–ammonia	4 beds	0.2–0.23	650 W/m^2	18–20	0.2
75	CPC	32.175	15 kW	Silica gel 47 kg	1 bed	–	963.89 W/m^2	–	0.3
98	FT	2	–	Silica gel 78.8 kg	1 bed	0.320	13–22 MJ/day m^2	–	0.1–0.25
110	Glass tube	–	6.9–9.4 kg/m^2	0.28 kg charcoal–methanol	1 bed	–	20 MJ/day m^2	13.6–15.9	0.46–0.50

COP: coefficient of performance; CPC: compound parabolic trough; FP: flat plate; VT: evacuated tube.

Conclusion

Solar thermal cooling method received significant interest in recent years. Utilizing solar cooling not only reduces electricity consumption but also reduces gas emission from fossil fuels and eliminates the harm effect of CFC and HCFC refrigerants. Solar cooling is a promising technology because solar radiation is in phase with the demand for cooling. This review article focuses on the recent developments in absorption and adsorption solar cooling systems. Detailed thermal analysis and economic assessment are provided.

Absorption method works in closed cycle and uses different liquid sorbents, but the most common refrigerant used is the LiBr–water pair. The highest COP achieved is 0.8 while the conventional cooling system can reach up to 3. However, absorption has the highest COP compared to other solar cooling technologies. The performance of the absorption cooling system depends on the heat and mass transfer, number of stages, number of beds, type of solar collector, cooling load schedule, control strategy, and capacity of the thermal storage. The high initial cost and low efficiency have motivated large number of studies aimed to overcome these drawbacks. The system efficiency can be improved by using high-temperature solar receiver, double-effect chiller, advanced control, and improved chiller efficiency.

Adsorption method works in closed cycle and uses different solid adsorption–desorption pairs. The performance of system depends mainly on the type of adsorption–desorption pairs, source temperature, adsorption chiller design, and operating condition. The long adsorption/desorption time, the size of the system, high cost of adsorption chillers, and low performance of the adsorption chiller prohibit significant commercial growth. The COP has reached 0.45 which is considered very low compared with any other cooling system. High COP and SCP can be achieved by increasing heat and mass recovery and by developing multi-stage, multi-bed technologies, and optimization operating conditions.

Up to now, the Pb of both the solar absorption and adsorption system exceeds the lifetime in large parts of the world. Hence, it is necessary to improve the performance of these systems. Absorption system has the highest market penetration among the solar cooling technology. The absorption chillers equipped with thermal energy storage system can provide cost-effective technical feasible solution for space cooling. The economic assessment revealed that the solar cooling system can be competitive only when using as double-purpose systems (heating and cooling systems) which have more COP than single-purpose systems. Finally, parabolic trough concentrators can significantly increase the solar cooling efficiency.

Declaration of conflicting interests

The authors declare that there is no conflict of interest.

Funding

This research received no specific grant from any funding agency in the public, commercial, or not-for-profit sectors.

References

1. Bataineh K and Fayez N. Thermal performance of building attached sunspace in Jordan climate. In: *The 1st international nuclear and renewable energy conference (INREC'10)*, Amman, Jordan, 21–24 March 2010, pp.1–6. New York: IEEE.
2. Bataineh K and Fayez N. Analysis of thermal performance of building attached sunspace. *Energ Build* 2011; 43: 1863–1868.
3. Bataineh K and Dalalah D. Optimal configuration for design of stand-alone PV system. *Smart Grid Renew Energ* 2012; 3: 2.
4. Bataineh K and Dalalah D. Assessment of wind energy potential for selected areas in Jordan. *Renew Energ* 2013; 59: 75–81.
5. Fong KF, Chow TT, Lee CK, et al. Comparative study of different solar cooling systems for buildings in subtropical city. *Sol Energ* 2010; 84: 227–244.
6. Chidambaram LA, Ramana AS, Kamaraj G, et al. Review of solar cooling methods and thermal storage options. *Renew Sust Energ Rev* 2011; 15: 3220–3228.
7. Enteria N, Yoshino H, Satake A, et al. Development and construction of the novel solar thermal desiccant cooling system incorporating hot water production. *Appl Energ* 2011; 87: 478–486.
8. Anyanwu EE. Review of solid adsorption solar refrigeration II: an overview of the principles and theory. *Energ Convers Manage* 2004; 45: 1279–1295.
9. Henning H-M. Solar assisted air conditioning of buildings—an overview. *Appl Therm Eng* 2007; 27: 1734–1749.
10. Qu, Yin H and Archer DH. A solar thermal cooling and heating system for a building: experimental and model based performance analysis and design. *Sol Energ* 2010; 84: 166–182.
11. Flechon J, Lazzarin R, Spinner B, et al. *Guild to solar refrigerators for remote areas and warm countries*. Paris: International Institute of Refrigeration (IIR), 1999.
12. Henning HM. *Solar-assisted air-conditioning in buildings, a handbook for planners*. Wien: Springer-Verlag, 2004.
13. Allouhi A, Kousksou T, Jamil A, et al. Solar driven cooling systems: an updated review. *Renew Sust Energ Rev* 2015; 44: 159–181.
14. Eicker U. *Low energy cooling for sustainable buildings*. Chichester: John Wiley & Sons, Ltd, 2009.
15. Duffie JA and Beckman WA. *Solar engineering of thermal process*. New York: A Wiley, Interscience Publications; Madison, WI: University of Wisconsin, 1980.
16. Budihardjo I, Morrison GL and Behnia M. Performance of a water-in-glass evacuated tube solar water heater. In: *Proceedings of solar—Australian and New Zealand solar energy society*, Newcastle, Australia, 27–29 November, 2002.
17. Atmaca I and Yigit A. Simulation of solar-powered absorption cooling system. *Renew Energ* 2003; 28: 1277–1293.
18. Boopathi Raja V and Shanmugam V. A review and new approach to minimize the cost of solar assisted absorption cooling system. *Renew Sust Energ Rev* 2012; 16: 6725–6731.
19. Somers C, Mortazavi A, Hwang Y, et al. Modeling water/lithium bromide absorption chillers in ASPEN Plus. *Appl Energ* 2011; 88: 4197–4205.
20. Hassan HZ and Mohamad AA. A review on solar cold production through absorption technology. *Renew Sust Energ Rev* 2012; 16: 5331–5348.
21. Casals XG. Solar absorption cooling in Spain: perspectives and outcomes from the simulation of recent installations. *Renew Energ* 2006; 31: 1371–1389.
22. Balghouthi M, Chahbani MH and Guizani A. Solar powered air conditioning as a solution to reduce environmental pollution in Tunisia. *Desalination* 2005; 185: 105–110.
23. Mazloumi M, Naghashzadegan M and Javaherdeh K. Simulation of solar lithium bromide–water absorption cooling system with parabolic trough collector. *Energ Convers Manage* 2008; 49: 2820–2832.
24. Sekret R and Turski M. Research on an adsorption cooling system supplied by solar energy. *Energ Build* 2012; 51: 15–20.
25. Eicker U and Pietruschka D. Design and performance of solar powered absorption cooling systems in office buildings. *Energ Build* 2009; 41: 81–91.
26. Yin YL, Song ZP, Li Y, et al. Experimental investigation of a mini-type solar absorption cooling system under different cooling modes. *Energ Build* 2012; 47: 131–138.
27. Pongtornkulpanicha A, Thepaa S, Amornkitbamrungb M, et al. Experience with fully operational solar-driven 10-ton LiBr/H_2O single-effect absorption cooling system in Thailand. *Renew Energ* 2008; 33: 943–949.
28. Hidalgo MCR, Aumente PR, Millan MI, et al. Energy and carbon emission savings in Spanish housing air-conditioning using solar driven absorption system. *Appl Therm Eng* 2008; 28: 1734–1744.
29. Helm M, Keil C, Hiebler S, et al. Solar heating and cooling system with absorption chiller and low temperature latent heat storage: energetic performance and operational experience. *Int J Refrig* 2009; 32: 596–606.
30. Hang Y, Du L, Qu M, et al. Multi-objective optimization of integrated solar absorption cooling and heating systems for medium-sized office buildings. *Renew Energ* 2013; 52: 67–78.
31. Tiago M and Oliveira AC. Energy and economic analysis of an integrated solar absorption cooling and heating system in different building types and climates. *Appl Energ* 2009; 86: 949–957.
32. Agyenim F, Knight I and Rhodes M. Design and experimental testing of the performance of an outdoor LiBr/H_2O solar thermal absorption cooling system with a cold store. *Sol Energ* 2010; 84: 735–744.

33. Llamas-Guillén SU, Cuevas R, Best R, et al. Experimental results of a direct air-cooled ammonia–lithium nitrate absorption refrigeration system. *Appl Therm Eng* 2014; 67: 362–369.
34. Lizarte R, Izquierdo M, Marcos JD, et al. An innovative solar-driven directly air-cooled LiBr–H_2O absorption chiller prototype for residential use. *Energ Build* 2012; 47: 1–11.
35. Lizarte R, Izquierdo M, Marcos JD, et al. Experimental comparison of two solar-driven air-cooled LiBr/H_2O absorption chillers: indirect versus direct air-cooled system. *Energ Build* 2013; 62: 323–334.
36. Iranmanesh A and Mehrabian MA. Dynamic simulation of a single-effect LiBr–H_2O absorption refrigeration cycle considering the effects of thermal masses. *Energ Build* 2013; 60: 47–59.
37. Kohlenbach P and Ziegler F. A dynamic simulation model for transient absorption chiller performance. Part I: the model. *Int J Refrig* 2008; 31: 217–225.
38. Kohlenbach P and Ziegler F. A dynamic simulation model for transient absorption chiller performance. Part II: numerical results and experimental verification. *Int J Refrig* 2008; 31: 226–233.
39. Izquierdo M, Venegas M, Rodriguez P, et al. Crystallization as a limit to develop solar air-cooled LiBr–H_2O absorption systems using low-grade heat. *Sol Energ Mater Sol Cell* 2004; 81: 205–216.
40. Sumathy K, Huang ZC and Li ZF. Solar absorption cooling with low grade heat source—a strategy of development in South China. *Sol Energ* 2002; 72: 155–165.
41. Grossman G. Solar-powered system for cooling, dehumidification and air conditioning. *Sol Energ* 2002; 72: 53–62.
42. Du S, Wang RZ, Lin P, et al. Experimental studies on an air-cooled two-stage NH_3-H_2O solar absorption air-conditioning prototype. *Energy* 2012; 45: 581–587.
43. Lin P, Wang RZ and Xia ZZ. Numerical investigation of a two-stage air-cooled absorption refrigeration system for solar cooling: cycle analysis and absorption cooling performances. *Renew Energ* 2011; 36: 1401–1412.
44. Domínguez-Inzunza LA, Hernández-Magallanes JA, Sandoval-Reyes M, et al. Comparison of the performance of single-effect, half-effect, double-effect in series and inverse and triple-effect absorption cooling systems operating with the NH_3–$LiNO_3$ mixture. *Appl Therm Eng* 2014; 66: 612–620.
45. Jawahar CP and Saravanan R. Generator absorber heat exchange based absorption cycle—a review. *Renew Sust Energ Rev* 2014; 14: 2372–2382.
46. Yari M, Zarin A and Mahmoudi SMS. Energy and exergy analyses of GAX and GAX hybrid absorption refrigeration cycles. *Renew Energ* 2011; 36: 2011–2020.
47. Velázquez N and Best R. Methodology for the energy analysis of an air cooled GAX absorption heat pump operated by natural gas and solar energy. *Appl Therm Eng* 2002; 22: 1089–1103.
48. Zheng D, Deng W, Jin H, et al. α–h diagram and principle of exergy coupling of GAX cycle. *Appl Therm Eng* 2007; 27: 1771–1778.
49. Xu ZY, Wang RZ and Xia ZZ. A novel variable effect LiBr–water absorption refrigeration cycle. *Energy* 2013; 60: 457–463.
50. Xu ZY and Wang RZ. Experimental verification of the variable effect absorption refrigeration cycle. *Energy* 2014; 77: 703–709.
51. Jayasekara S and Halgamuge SK. Mathematical modeling and experimental verification of an absorption chiller including three dimensional temperature and concentration distributions. *Appl Energ* 2013; 106: 232–242.
52. Chua HT, Toh HK and Ng KC. Thermodynamic modeling of an ammonia–water absorption chiller. *Int J Refrig* 2002; 25: 896–906.
53. Ben Ezzine N, Barhoumi M, Mejbri Kh, et al. Solar cooling with the absorption principle: first and second law analysis of an ammonia—water double-generator absorption chiller. *Desalination* 2004; 168: 137–144.
54. Hang Y, Qu M and Ukkusuri S. Optimizing the design of a solar cooling system using central composite design techniques. *Energ Build* 2011; 43: 988–994.
55. Assilzadeh F, Kalogirou SA, Ali Y, et al. Simulation and optimization of a LiBr solar absorption cooling system with evacuated tube collectors. *Renew Energ* 2005; 30: 1143–1159.
56. Lecuona A, Ventas R, Venegas M, et al. Optimum hot water temperature for absorption solar cooling. *Sol Energ* 2009; 83: 1806–1814.
57. Marc O, Praene JP, Bastide A, et al. Modeling and experimental validation of the solar loop for absorption solar cooling system using double-glazed collectors. *Appl Therm Eng* 2011; 31: 268–277.
58. Joudi KA and Abdul-Ghafour QJ. Development of design charts for solar cooling systems. Part I: computer simulation for a solar cooling system and development of solar cooling design charts. *Energ Convers Manage* 2003; 44: 313–339.
59. Palacin F, Monne C and Alonso S. Improvement of an existing solar powered absorption cooling system by means of dynamic simulation and experimental diagnosis. *Energy* 2011; 36: 4109–4118.
60. Eicker U, Pietruschka D and Pesch R. Heat rejection and primary energy efficiency of solar driven absorption cooling systems. *Int J Refrig* 2012; 35: 729–738.
61. Bhardwaj PK, Kaushik SC and Jain S. General performance characteristics of an irreversible vapour absorption refrigeration system using finite time thermodynamic approach. *Int J Therm Sci* 2005; 44: 189–196.
62. Fathi R, Guemimi C and Ouaskit S. An irreversible thermodynamic model for solar absorption refrigerator. *Renew Energ* 2004; 29: 1349–1365.
63. Hamza A, Ali H, Noeres P, et al. Performance assessment of an integrated free cooling and solar powered single-effect lithium bromide-water absorption chiller. *Sol Energ* 2008; 82: 1021–1030.
64. Balghouthi M, Chahbani MH and Guizani A. Feasibility of solar absorption air conditioning in Tunisia. *Build Environ* 2008; 43: 1459–1470.
65. Dawoud B. A hybrid solar-assisted adsorption cooling unit for vaccine storage. *Renew Energ* 2007; 32: 947–964.

66. Syed A, Izquierdo M, Rodrıgueze P, et al. A novel experimental investigation of a solar cooling system in Madrid. *Int J Refrig* 2005; 28: 859–871.
67. Monne C, Alonsa S, Palacin F, et al. Monitoring and simulation of an existing solar powered absorption cooling system in Zaragoza (Spain). *Appl Therm Eng* 2011; 31: 28–35.
68. Marc O, Lucas F, Sinama F, et al. Experimental investigation of a solar cooling absorption system operating without any backup system under tropical climate. *Energ Build* 2010; 42: 774–782.
69. Ghaddar NK, Shihab M and Bdeir F. Modeling and simulation of solar absorption system performance in Beirut, 1996. *Renew Energ* 1997; 10: 539–558.
70. Jaruwongwittaya T and Chen G. A review: renewable energy with absorption chillers in Thailand. *Renew Sust Energ Rev* 2010; 14: 1437–1444.
71. Shekarchian M, Moghavyemi M, Mostasemi F, et al. Energy saving and cost benefit analysis of using compression and absorption chiller for air conditioners in Iran. *Renew Sust Energ Rev* 2011; 15: 1950–1960.
72. Trygg L and Amiri S. European perspective on absorption cooling in combine heat and power system—a case study of energy utility and industries in Sweden. *Appl Energ* 2007; 84: 1319–1337.
73. Tsoutsos T, Anagnostou J, Pritchard C, et al. Solar cooling technologies in Greece. An economic viability analysis. *Appl Therm Eng* 2003; 23: 1427–1439.
74. Elsafty A and Al-Daini AJ. Economical comparison between a solar powered vapour absorption air-conditioning system and a vapour compression system in the Middle East. *Renew Energ* 2002; 25: 569–583.
75. Gebreslassie BH, Guillen-Goslbez G, Jimenez L, et al. A systematic tool for the minimization of the life cycle impact of solar assisted absorption cooling systems. *Energy* 2010; 35: 3849–3862.
76. Mehr AS, Zare V and Mahmoudi SMS. Standard GAX versus hybrid GAX absorption refrigeration cycle: from the view point of thermoeconomics. *Energ Convers Manage* 2013; 76: 68–82.
77. Askalany AA, Saha BB, Kariya K, et al. Hybrid adsorption cooling systems—an overview. *Renew Sust Energ Rev* 2012; 16: 5787–5801.
78. Zhai XQ and Wang RZ. Experimental investigation and theoretical analysis of the solar adsorption cooling system in a green building. *Appl Therm Eng* 2009; 29: 17–27.
79. Lambert MA and Beyene A. Review of solid adsorption solar refrigerator I: an overview of the refrigeration cycle. *Energ Convers Manage* 2003; 44: 301–312.
80. Dai YJ, Sumathy K, Wang RZ, et al. Enhancement of natural ventilation in a solar house with a solar chimney and a solid adsorption cooling cavity. *Sol Energ* 2003; 74: 65–75.
81. Amanul Alam KC, Saha BB and Akisawa A. Adsorption cooling driven by solar collector: a case study for Tokyo solar data. *Appl Therm Eng* 2011; 50: 1–7.
82. Alghoul MA, Sulaiman MY, Sopian K, et al. Performance of a dual-purpose solar continuous adsorption system. *Renew Energ* 2009; 34: 920–927.
83. Chang WS, Wang CC and Shieh CC. Experimental study of a solid adsorption cooling system using flat-tube heat exchangers as adsorption bed. *Appl Therm Eng* 2007; 27: 2195–2199.
84. Alghoul MA, Sulaiman MY, Azmi BZ, et al. Advances on multi-purpose solar adsorption systems for domestic refrigeration and water heating. *Appl Therm Eng* 2007; 27: 813–822.
85. Wang DC, Li YH, Li D, et al. A review on adsorption refrigeration technology and adsorption deterioration in physical adsorption systems. *Renew Sust Energ Rev* 2010; 14: 344–353.
86. Anyanwu EE and Ogueke NV. Thermodynamic design procedure for solid adsorption solar refrigerator. *Renew Energ* 2005; 30: 81–96.
87. Luo HL, Dai YJ, Wang RZ, et al. Experimental investigation of a solar adsorption chiller used for grain depot cooling. *Appl Therm Eng* 2006; 26: 1218–1225.
88. Sumathy K, Yeung KH and Yong Li. Technology development in the solar adsorption refrigeration systems. *Prog Energ Combust* 2003; 29: 301–327.
89. Hassan HZ, Mohamad AA and Al-Ansary HA. Development of a continuously operating solar-driven adsorption cooling system: thermodynamic analysis and parametric study. *Appl Therm Eng* 2012; 48: 332–341.
90. Critoph RE. Forced convection adsorption cycle with packed bed heat regeneration. *Int J Refrig* 1999; 22: 38–46.
91. Zhai XQ and Wang RZ. Experimental investigation and performance analysis on a solar adsorption cooling system with/without heat storage. *Appl Energ* 2010; 87: 824–835.
92. Ge TS, Li Y, Dai YJ, et al. Performance investigation on a novel two-stage solar driven rotary desiccant cooling system using composite desiccant materials. *Sol Energ* 2010; 84: 157–159.I.I,
93. Wang RZ and Oliveira RG. Adsorption refrigeration—an efficient way to make good use of waste heat and solar energy. *Prog Energ Combust* 2006; 32: 424–458.
94. Saha BB, El-Sharkawy II, Chakraborty A, et al. Study on an activated carbon fiber–ethanol adsorption chiller: part I—system description and modeling. *Int J Refrig* 2007; 30: 86–95.
95. Yong L and Sumathy K. Review of mathematical investigation on the closed adsorption heat pump and cooling systems. *Renew Sust Energ Rev* 2002; 6: 305–337.
96. Maggio G, Gordeeva LG, Freni A, et al. Simulation of a solid sorption ice-maker based on the novel composite sorbent "lithium chloride in silica gel pores". *Appl Therm Eng* 2009; 29: 1714–1720.
97. Li M, Huang HB, Wang RZ, et al. Experimental study on adsorbent of activated carbon with refrigerant of methanol and ethanol for solar ice maker. *Renew Energ* 2004; 29: 2235–2244.
98. Hildbrand C, Dind P, Pons M, et al. A new solar powered adsorption refrigerator with high performance. *Sol Energ* 2004; 77: 311–318.
99. Vasta S, Maggio G, Santori G, et al. An adsorptive solar ice-maker dynamic simulation for north Mediterranean climate. *Energ Convers Manage* 2008; 49: 3025–3035.
100. Al Mers A, Azzabakh A, Mimet A, et al. Optimal design study of cylindrical finned reactor for solar

adsorption cooling machine working with activated carbon–ammonia pair. *Appl Therm Eng* 2006; 26: 1866–1875.
101. Louajari M, Mimet A and Ouammi A. Study of the effect of finned tube adsorber on the performance of solar driven adsorption cooling machine using activated carbon–ammonia pair. *Appl Energ* 2011; 88: 690–698.
102. Abu-Hamdeh NH, Alnefaie KA and Almitani KH. Design and performance characteristics of solar adsorption refrigeration system using parabolic trough collector: experimental and statistical optimization technique. *Energ Convers Manage* 2013; 74: 162–170.
103. Liu Y and Leong KC. The effect of operating conditions on the performance of zeolite/water adsorption cooling systems. *Appl Therm Eng* 2005; 25: 1403–1418.
104. Liu Y and Leong KC. Numerical modeling of a zeolite/water adsorption cooling system with non-constant condensing pressure. *Int Commun Heat Mass Tran* 2008; 35: 618–622.
105. Khattab M. A novel solar-powered adsorption refrigeration module. *Appl Therm Eng* 2004; 24: 2747–2760.
106. Abu Hamdeh NH and Al-Muhtaseb MA. Optimization of solar adsorption refrigeration system using experimental and statistical techniques. *Energ Convers Manage* 2010; 51: 1610–1615.
107. Khana MZI, Saha BB, Alam KCA, et al. Study on solar/waste heat driven multi-bed adsorption chiller with mass recovery. *Renew Energ* 2007; 32: 365–381.
108. Lambert MA. Design of solar powered adsorption heat pump with ice storage. *Appl Therm Eng* 2007; 27: 1612–1628.
109. Xu S. Simulation on a new adsorption bed about adsorption refrigeration driven by solar energy. *Proced Eng* 2011; 15: 3865–3869.
110. Khattab NM. Simulation and optimization of a novel solar-powered adsorption refrigeration module. *Sol Energ* 2006; 80: 823–833.
111. Luo HL, Wang RZ, Dai YJ, et al. An efficient solar-powered adsorption chiller and its application in low-temperature grain storage. *Sol Energ* 2007; 81: 607–613.
112. Li S and Wu JY. Theoretical research of a silica gel–water adsorption chiller in a micro combined cooling, heating and power (CCHP) system. *Appl Energ* 2009; 86: 958–967.

Appendix I

Notation

A_C	area solar collector (m)
C_c	capital cost of installed solar cooling equipment (€)
C_p	specific heat at constant pressure (J/kg K)
C_v	specific heat at constant volume (J/kg K)
C_{vw}	water-specific heat (J/kg K)
$\Delta C_{annual,sol}$	annual extra cost for solar plant
E	energy saving (€/year)
F_R	flow ratio
h	specific enthalpy (J/kg)
h_{fg}	latent heat of vaporization (J/kg)
H	extensive enthalpy (J)
I	energy inflation (the change in energy prices relative to general inflation)
I_s	solar insulation
L	life period (year)
L_i	daily cooling load (kW)
m	mass flow rate (g/s)
M	total mass (kg)
P	pressure (Pa)
Q	heat flow across heat exchanger (W)
Q_{aux}	auxiliary heater capacity (kW)
Q_L	extracted energy from the storage tank (kW)
Q_u	useful collected energy (kJ)
Q_∂	nominal capacity of the chiller (kW)
r	market discount rate
s	specific entropy (J/g K)
S	extensive entropy (J/K)
T	temperature/temperature of solution (°C)
T_a	ambient temperature (°C)
T_c	condenser temperature
T_e	evaporator temperature
T_{fi}	inlet fluid temperature (K)
T_{fo}	outlet fluid temperature (K)
T_g	generator temperature
T_i	interfacial temperature (°C)
T_{in}	collector inlet temperature (°C)
T_{pm}	plate mean temperature (K)
T_s	storage temperature
U	overall heat transfer coefficient ($W/m^2 K$)
U_L	overall heat loss coefficient ($W/m^2 K$)
X	mass concentration of NH_3 or LiBr in solution
Xi	interfacial liquid mass concentration of NH_3 or LiBr
y	mass concentration of NH_3 in vapor
y_i	interfacial vapor mass concentration of NH_3 or LiBr
Y	yearly benefits (€/year)
Ym	molar concentration of NH_3 in vapor
z	film thickness (m)
α	heat diffusivity (m^2/s)
η_c	collector efficiency
$\tau\alpha$	effective absorptance–transmittance product
χ	LiBr mass fraction
ω	adsorption uptake

Subscripts

a	*adsorbent bed*
abs	absorber
amb	ambient
chill	chilled water

cond	condenser
des	desorber
evap	evaporator
gen	generator
gc	glass cover or saturation gas
i	inlet
o	outlet
ref	refrigerant
sol	solution
vap	vapor
w	water